Micromechanical Analysis of Thermoplastic - Thermoset Interphase

J. M. Vazquez-Rodríguez, P. J. Herrera-Franco, P. I. Gonzalez-Chi*

Centro de Investigación Científica de Yucatán, AC, Unidad de Materiales, Calle 43, No. 130, col. Chuburná de Hidalgo 97200, Mérida, Yucatán, México
E-mail: ivan@cicy.mx

Summary: The interfacial shear strength of a pull out model between a thermoplastic fiber and thermoset matrix was analyzed. The method to analyze the interfacial quality in this kind of composite was Photoelasticity. The interfacial shear strength was measured localizing the isocromatic fringes. The Isochromatic fringe corresponds to the points along the specimen in which the principal stresses have the same value.

Keywords: composites; interfacial shear strength; photoelasticity; polyesters; pull out

Introduction

Photoelasticity is a well-established technique for stress analysis and has a wide range of industrial and research applications. The main goal of this technique is the determination of isoclinic and isochromatic fringes to analyze the shear stress and stress distribution in a sample [1, 2]. The light used for the analysis can be white or a bean with only some monochromatic lines. In the first case, the analysis generates an image with a full decomposition of wavelengths in which, each one corresponds to a level of shear strength. It is easer to recognize the phase change for the image analysis of the shear strength when a narrow-chromatic light is used [3].

Photoelasticity has been used to study the shrinkage process of resins used for medical items. To understand this phenomenon, could improve composite elaboration for clinical effectiveness [4, 5].

A photoelastic experimental method has been used for analyzing the stress at the vicinity of crack tips and, in conjunction with the theory of Shear Lag, the stress fields between a short-fiber and the matrix in composites were described [6, 7, 8, 9]. Photoelasticity is a common way

 DOI: 10.1002/masy.200451213

for testing a single fiber composite. The analysis gives the opportunity to follow *in-situ* their failure mechanics like fiber debonding, fibre breaks, matrix fracture and matrix yield [10].

Wang Feng and Xie Himin [11] made a strain analysis for materials with different elastic modulus using the method of the shear stress difference to calculate the interfacial strength. The model was based on the experimental solution of the stress tensor obtained from an interphase deformed continuous conditions, reducing the tensor to a plane problem, by vertical projection of one of the stress components. For the analysis models for the axial and transversal direction were needed [11].

Photoelasticity was also used for monitoring the failure process due the humidity in carbon fiber and epoxy resin composites [12]. Heterogeneous fibre composites were studied and it was found that the specimen had an equivalent birefringence and an equivalent birefringence direction to the addition of the different fibre distribution [13, 14].

Some other studies used an interferometric technique for photoelastic testing to detect the spatial deformation of the stressed specimen and hence the spatial strain distributions. This study concluded that the maximum stressed zones are those were the maximum fringe distortion occurs [15, 16]. A. Tomlinson and E. A. Paterson [17] used a different method to analyze the shear strength. They used a step-wise loading system and the model was sectioned into discrete imaginary-slices and a relationship was derived between the retardation and the isoclinic angle [17].

There had been attempts to digitalize and process the images with software to obtain reconstructed theoretical fringe patterns from a loading frame in a polarization bench [18, 19]. Nevertheless it requires frame recorders and some other equipment that makes the process complicated.

Polarization

A plane beam is obtained using a polariscope, which consists of a light source and two polarization elements with the polarization axis crossed. A single light beam composed of a large number of randomly oriented waves, propagates following a harmonic motion along a straight line [20, 21]. Polarization fixes the light beam propagation in only single plane. The photoelastic patterns can be obtained with a plane or a circular polariscope, and the light intensity (I) emerging is:

$$I = E^2 sen^2 2\alpha \; sen^2 \frac{R}{2} \qquad (1)$$

The equation (1) represents the dark field of a plane polariscope in which I is function of the angle between the normal and the principal stress direction (α) and the relative retardation (R) induced when the light beam passes through the stressed specimen. There are two conditions in which I is zero (the light beam is extinguished). The first one is when the angle of the principal stress directions corresponds to α_i= 0, $\pi/2$,π, $3\pi/2$ . . . radians and the second condition is when the relative retardation corresponds to R= 0, 2π . . . $N\pi$ radians, where N is an integer. N represents the number of complete wavelengths or retardation cycles produced by an induced strain and it is called isochromatic fringe.

When the polariscope axis coincides with the principal stress direction (α) a dark fringe is obtained. This fringe corresponds to the points along which the principal stresses have parallel directions and it is known as isoclinic fringe [21].

In the case of the isochromatic order N, when a complete cycle of retardation is reached, it produces another dark fringe called an isochromatic fringe which is directly related to the shear strength. N is known as photoelastic order, fringe order or isochromatic order. The isochromatic fringes are easier to obtain using a circular polarization, which is obtained by adding two-quarter wave elements to a plane polariscope. The light intensity I emerging from this polariscope is:

$$I = E_y^2 (1 - \cos R)$$

$$I = 2E_y^2 sen^2 \frac{R}{2}$$

$$I = K sen^2 \frac{R}{2} \qquad (2)$$

Where K is a constant for each polariscope. This equation has the following extinction conditions for the fringe order N:

$$I = 0 \qquad for \quad \frac{R}{2} = 0, \pi ... radians \quad or \quad R = 0, 2\pi ...., N(2\pi)$$

When the relative strain induces a retardation of N_i= 1, 2, 3 . . . a dark isochromatic fringe is obtained. The stress optic law [20] is commonly written as:

$$\sigma_1 - \sigma_2 = \frac{N f_\sigma}{h_L} \qquad (3)$$

where $N = R/2\pi = \delta/\lambda$ is the relative retardation in terms of complete cycles N and depends from the wavelength (λ). h_L is the distance traveled by the light in the stressed specimen. $f_\sigma = \lambda/C$ is the material fringe value or fringe-stress coefficient. And C is the ratio between the relative stress-optic coefficients of each material.

The shear strength is defined by the following equation:

$$\frac{\sigma_1 - \sigma_2}{2} = \frac{Nf_\sigma}{2h_L} = \tau_{Max} \quad (4)$$

Photoelastic Calibration

The photoelastic calibration of the epoxy resin was made using the four points bending method. This method produces stress patterns of pure bending: The beam has no vertical stress (σ_y), transverse normal stress (σ_x) or horizontal shear stresses (τ_{xy}).

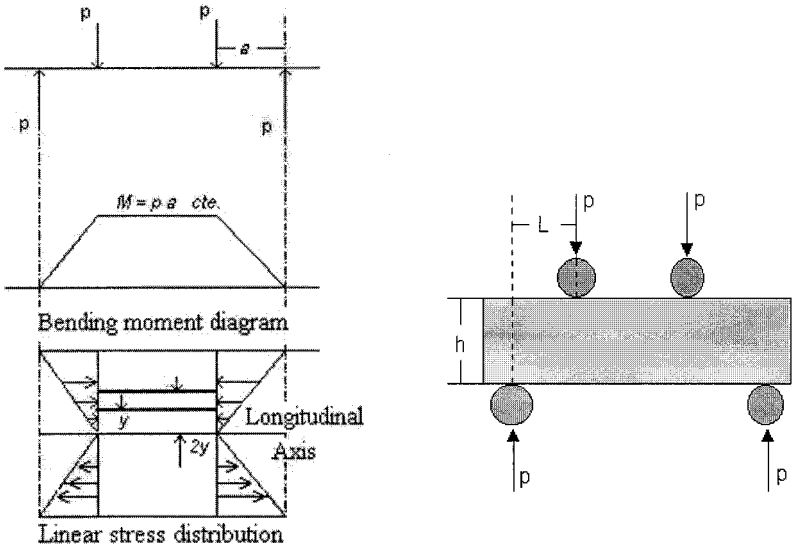

(a) (b)

Figure 1. Bending moment diagram, linear stress distribution (a), of four points-bending set up (b).

The equation used for the epoxy resin calibration was:

$$f_\sigma = \frac{3Pa}{h^2 N} \quad (5)$$

Where P is the load in Newton, a is the length between supports in meter, h is the beam height in meter, N is the photo elastic order and f_σ is the fringe-stress coefficient in Newton per meters.

Pull-out Test

The micromechanic technique used was the Pull-out test in which one end of a filament is embebed in a matrix block and the filament free end is loaded. The applied load and the displacement are continuously monitored until the filament is extracted or the interphase fails. The stress analysis is made considering a balance between the tension stress at the fiber (σ_f) and the shear stress (τ) at the interphase [3]. The Pull-out test has been used to measure the adhesion between two different materials[22, 23] and it is widely used to measure the shear strength at the interphase between a fibre and an epoxy-matrix[24, 25, 26].

Materials

The Pull-out specimens were manufactured using a bisphenol-A epoxy resin DER 331 from DOW Química Mexicana S. A. The curing agent was an aliphatic diamine ANCAMINE 1784 from Air Products and Chemicals, Inc. The thermoplastic polyester fiber was from KIRSCHBAUM.

Experimental

The fiber tensile test was performed according to the ASTM D2343-67 using a universal test machine Shimatzu A 61 fitted with a 5 kN load cell at 30 mm/min with a gauge length of 245 mm.

The tensile test of the epoxy resin was made using the ASTM D 638-82[a] in the universal test machine Shimatzu A 61 with a load cell of 5 kN, gauge length of 50 mm. The testing speed was 1 mm/min. The Poisson ratio was measured according to the ASTM D 638-82[a] with two extensometric gauges (EA-06250 BF-350 gauge factor 2.095 ± 0.5%) cemented perpendicularly to each one along the main specimen axis. The test was in a step-wise loading fashion at the elastic zone of the epoxy resin.

To calculate the Poisson ratio the equation used was:

$$\nu_{yx} = -\frac{\varepsilon_x}{\varepsilon_y} \quad (6)$$

Where ν_{xy} is the Poisson ratio, ε_x and ε_y are the strains in the axial and transversal directions respectively.

Polariscope Arrangement

The polarization instrument was arranged as follows to conform a circular polariscope. Two polarization elements crossed 90°. Two quarter-wave elements displaced ± 45° to the polarization axis of the first polarization element. The light emission was obtained form a mercury bulb with a wavelength of 540 nm. The load was transmitted to the specimen using a load frame with a cantilever system.

Specimen Preparation

The epoxy resin specimen for the optical calibration was 1.0 cm wide, 10.0 cm long and 0.5 cm thick. The pull-out specimen had the following dimensions: The resin block was 4 cm wide, 6 cm long and 1.1 cm thick. The fiber was longitudinally embebed at the center of the block, and the embebed length was of 4 cm. The free length of the fiber was 3 cm. The curing process took place for eight days under controlled humidity conditions at room temperature.

Results and Discussion

The tensile properties of the fiber are shown at Table 1 and for the epoxy resin al Table 2.

Table 1. Tensile characteristics of the polyester fiber.

	Elastic module	**Strength**	**Max. Strain**	**Failure stress**
	MPa	MPa	%	MPa
Average	6003.61	576.779	46.6248	568.637
SD	1.7078	1.7078	1.7078	1.7078

Table 2. Tensile properties of the Epoxy resin.

	Elastic Module	Strength	Max Strain	Poisson ratio
Specimen	MPa	MPa	%	
Average	1032.050	22.7621	9.3126	0.3840
SD	2.5819	2.5819	2.5819	1.8708

The ratio between the elastic module of the fiber and the epoxy resin is around 6, which is enough to get the isochromatic response from the specimens maintaining the elastic behavior of the fiber.

The epoxy resin had an average Poisson ratio of 0.3840. The performance of the epoxy resin block with this Poisson ratio generates a radial compression stress on the fiber during the load process. In the present analysis, the compression stress was not measured and considered low. To analyze the performance of the compression stress in a Pull-out specimen and to understand how affects the failure process it is necessary to analyze the directions of the principal stress.

Photoelastic Calibration of the Epoxy-resin.

Figure 2 shows a picture sequence from the four points bending test. They show the increase of the shear strength at the specimen as an increase on isochromatic fringes.

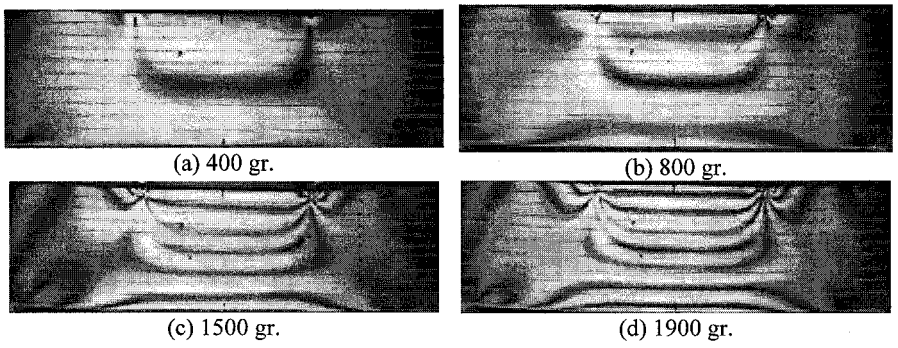

Figure 2. Photoelastic fringes of a circular polariscope (dark plane) in a four points bending system. The applied load is below each picture. The photoelastic order
(a) zero, (b) one, (c) two and (c) three.

From the pictures the photoelastic fringe stress-coefficient f_σ was obtained. The dark fringe at the center is the zero photoelastic order; the upper photoelastic orders were counted from the center to the sides.

Figure 3 shows the plot of $3Pa$ vs. h^2N. The slope is the f_σ. coefficient according the equation 5. Five specimens were tested and f_σ was calculated (Table 3), its average value is f_σ = 2,432.62 N/m (SD = 65.89).

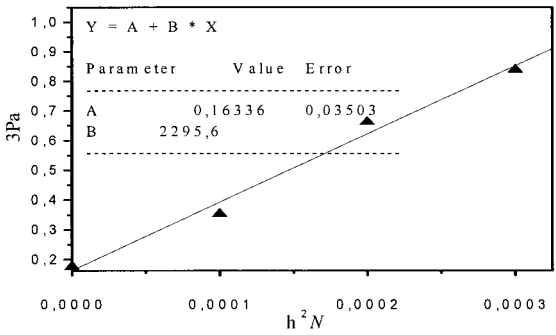

Figure 3. Equation 5 plot to calculate the fringe-stress coefficient f_σ which is the slope of the lineal regression.

Table 3. Fringe-stress coefficient f_σ for specimen 1.

Specimen 1	h = 1 cm		a = 1.5cm		
Weight grams	Load P Newton	Photoelastic Order (N)	3Pa	h^2N	Fringe stress Coefficient f_σ. (slope)
400	3.92	0	0.1766	0	
800	7.85	1	0.3532	0.0001	
1500	14.72	2	0.6622	0.0002	2295.6
1900	18.64	3	0.8388	0.0003	

Shear Strength by Photoelasticity

The strain transmitted from the fiber to the resin block gave us the opportunity to monitor the interphase failure process, which can be divided in three principal steps. The initial step did no show any photoelastic response. An incipient response was obtained when the minimum load used was 400 gr. The following step was the shear strength growth. During this step before of

the interphase failure two photoelastic fringes were obtained.

The pictures used to measure the shear strength between the fiber and the epoxy resin blocks are shown at the Figure 4.

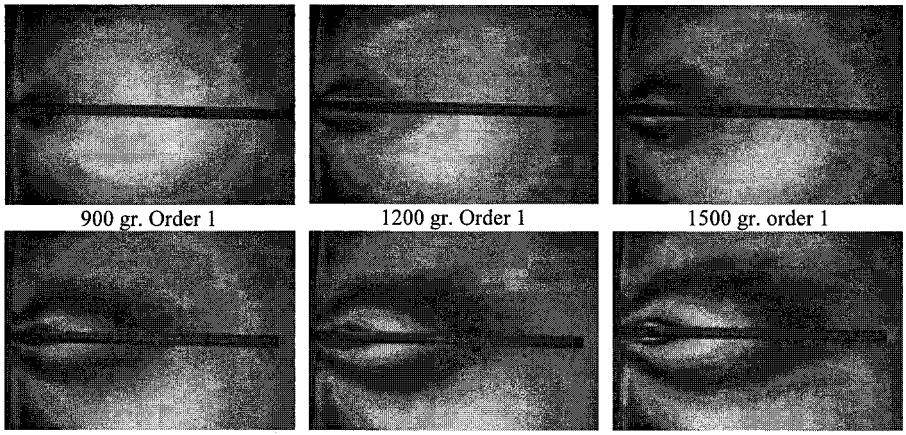

Figure 4. Isochromatic fringes for different loads (dark plane of a circular polariscope).

These pictures are from the loaded Pull out specimens. The beginning and the end of the photoelastic fringe mark the field where the shear strength acts over the fibre. The shear strength is related to the fringe order and it is maximum at the left side at the block where the fiber emerges from the epoxy resin. For that reason the second order fringe (small fringe close to the fiber) appears on that region. The maximum shear strength begins at this area where the free fiber was loaded. From 900 gr. to 1500 gr. the development of the first photoelastic order (N_f=1) is shown. When the load reaches 1900 gr., the second photoelastic order (N_f=2) appears. The second photoelastic order is directly related to higher shear strength, and acts over the same points of the epoxy resin block where the first photoelastic order was before. The growing of the second photoelastic order conduced to the interphase failure; only two photoelastic orders were obtained. The maximum load that the specimens supported before the interphase failure was of 2400 gr. The shear stress for each specimen was calculated using the equation 4.

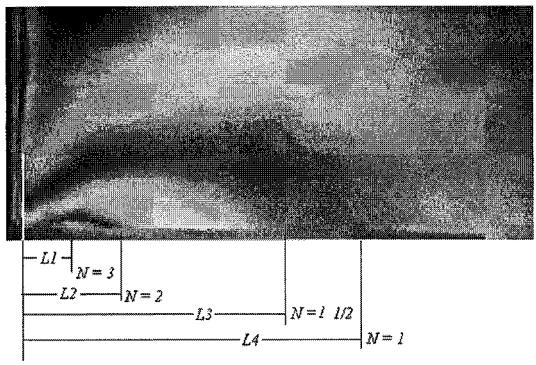

Figure 5. Measuring and location of photoelastic fringes.

Five specimens were tested to measure the photoelastic shear strength. The loads used were from 400 gr. to 2400 gr. To measure the shear strength rise, two photoelastic orders from the dark field and three from the bright field were obtained. The images of the dark field were obtained directly from the polariscope, and the images form the bright field were the negative image of the dark field. The dark fringes in these images represent the half-photoelastic orders of the bright field. The half orders obtained were: ½, 1 ½ and 2½ orders. These five orders (Table 4) were used to find the τ_{Max} distribution along the fiber as is shown in the Figure 5.

Table 4. Shear stress for the specimen 1.

Specimen 1 h_L = 5.5 mm		Fringe stress Coefficient f_σ. = 2427.900 N/m	
Photoelastic order N	$(\sigma_1 - \sigma_2) = 2\,\tau_{Max}$ Strength (Pa)	$\tau_{Max} = N f_\sigma / 2h_L$ Shear strength (Pa)	Longitud on the fiber affected by the τ_{Max} L(cm)
0.50	220718.182	110359.091	3.7053
1.00	441436.364	220718.182	2.9413
1.50	662154.545	331077.273	1.4576
2.00	882872.727	441436.364	1.0152
2.50	1103590.909	551795.455	0.6595

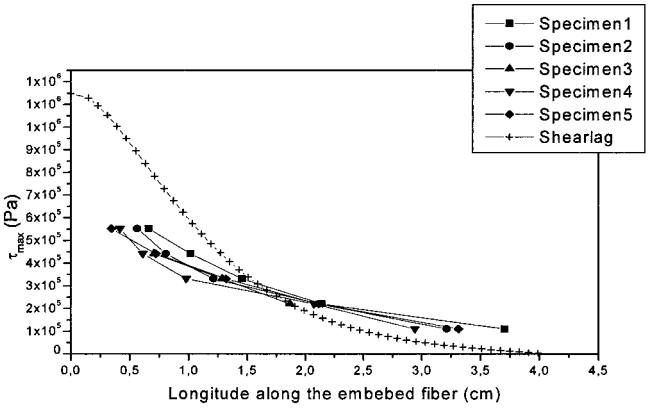

Figure 6. Shear strength distribution along the embebed fibre of the Pull-outspecimen analyzed by photoelasticity.

Figure 6 shows the shear strength distribution from the Shear lag theory and experimental results. The length along which the shear strength acts was measured from the beginning of the photoelastic order at the left side of the pictures (fiber section) to its end in the epoxy resin block. τ_{Max} acting over the section from 0.25 to 0.70 cm from the border over the embebed fiber for photoelastic test. The maximum Photoelastic shear strength is located about 0.5 cm from the border of the specimen. After this maximum, the shear strength decreases towards the embebed end of the fiber.

The performance of the photoelastic Shear strength versus Shear lag follows almost the same trajectory except close to the free fiber section and at the embebed tip where the Shear lag theory do not takes in count variables like the adhesion at the end of the embebed fiber or the complex loads close to the free fiber section.

Conclusions

The photoelastic technique relates the strains with the interfacial shear strength in a Pull out specimen under a load. The isocromatic fringes obtained from a Pull-out specimen were used to measure the interfacial shear strength and in spite of this, we can measure the maximum shear strength for a thermoplastic-thermoset interphase.

The load process of the Pull-out specimens was followed in real time. It made possible to see the initial load and the strength transfer from the fiber to the epoxy resin block. That effect was shown earlier. Where, the initial load was followed for a growing of the strain. The shear strength form the initial strain to the extraction of the embebed-fiber was shown by the isochromatic fringe.

The mechanical characteristics of the embebed fiber and the epoxy resin were different. The elastic module of the fiber was 6003.61 MPa and the module of the epoxy resin was 1032 N/mm^2. This difference helped to strain the epoxy resin and to obtain the photoelastic fringes while the fiber acted as an elastic rod. The Poisson ratio of the epoxy resin was of 0.38403.

The isochromatic fringes for a four point bending system were obtained with a dark field and it was reproducible. The point in which each fringe order was located is important; if the fringe order was located in a different point it conduces to an error of the epoxy-calibration. The photoelastic calibration of the epoxy resin was made and the fringe-stress coefficient f_σ had an average value of 2,427.9 N/m.

There were a good concordance between the Shear lag theory and the photoelastic experiment and the experimental results from the photoelastic experiments were reproducible for all the specimens tested.

[1] J. A. Quiroga, A. Gonzalez Cano, *Solid Mechanics Solid Mechanics and Its Applications* **2000**, *82*, 17.
[2] J. A. Quiroga, A. Gonzalez Cano, *Applied Optics* **2000**, *39*, 2931.
[3] S Yoneyama, M. Shimizu, *Optics and Lasers in Engineering* **1998**, *29*, 423.
[4] Y. Kinomoto, M. Torij, *Journal of Dentistry* **1998**, *26*, 165.
[5] Hassan M. Ziada, John F. Orr, *The journal of Prosthetic Dentistry* **1998**, *80*, 661.
[6] J.-S. Hawong, J.-G. S. Kyungdong, Yeungnam University; Kyungdong Junior College VIII International Congress on Experimental Mechanics Nashville, Tennessee, USA, 10-13 June **1996**
[7] P. J. Withers, E.M. Chorley, T. W. Clyde, *Materials Science and Engineering A* **1991**, *13* ,5173.
[8] S. Ritter, Busse, Plenum Publishing Corp., Review of Progress in Quantitative Nondestructive Evaluation. Volume 17B USA **1998**, 1201.
[9] J. Hobbs, R. Burguete, *Journal of Strain Analysis* **2000**, *36*, 93.
[10] S. Ritter, Busse Plenum Publishing Corp., Review of Progress in Quantitative Nondestructive Evaluation. Volume 17B USA **1998**, 1201.
[11] W. Feng, X. Himin, *Journal of Material Processing Technology* **1997**, *65*, 165.
[12] Z. R. Xu, K. H. G. Ashbee, *Int. Journal of Materials Science* **1994**, *2*, 394.
[13] W. Zhang, Y. Wan, *Int. Journal of Mechanical Science* **1995**, *37*, 933.
[15] K. Bhattacharya, A. Basuray, *Optics Communication* **1994**, *109*, 380.
[16] S. Yoneyama, M. Takashi, *Optics and Lasers in Engineering* **1998**, *30*, 441.
[17] A. Tomlinson, E. A. Patterson, *Journal of Strain Analysis* **1999**, *34*, 295.
[18] A. Ajovalasit; S. Barone; G. Petrucci, *Journal of Strain Analysis for Engineering Design*, **1998**, *33*, 75.
[19] J. A. Quiroga; A. Gonzalez Cano, *Applied Optics* **1997**, *36*, 8397.
[20] C. P. Burger, A. S. Kobayashi, "*Photoelasticity*" cap 5 Handbook of Experimental Mechanics second revised edition **1993.**
[21] M. M. Frocht, Ph. D. "*Photoelasticity*"Vol. I John Wiley and Sons, Inc. New York, **1947.**

[22] P. J. Herrera Franco V. Rao, L. T. Drzal, *Composites* **1992**, *23*, 2.
[23] M. R Piggott, *Composites Science and technology* **1987**, *30*, 295.
[24] J. A. Nairn, H. D. Wagner, *Material Science and Engineering Mechanics of Materials* **1997**, *26*, 63.
[25] L.B Greszczuc,. Composites ASTM STP 452, ASTM **1969**
[26] P. Laurence, *Journal of Materials Science* **1972**, *7*, 1.